DOI: 10.1002/cphc.200700700

Alkali Metal Complexes of the Dipeptides PheAla and AlaPhe: IRMPD Spectroscopy**

Nick C. Polfer,[b] Jos Oomens,[c] and Robert C. Dunbar*[a]

Complexes of PheAla and AlaPhe with alkali metal ions Na^+ and K^+ are generated by electrospray ionization, isolated in the Fourier-transform ion cyclotron resonance (FT–ICR) ion trapping mass spectrometer, and investigated by infrared multiple-photon dissociation (IRMPD) using light from the FELIX free electron laser over the mid-infrared range from 500 to 1900 cm^{-1}. Insight into structural features of the complexes is gained by comparing the obtained spectra with predicted spectra and relative free energies obtained from DFT calculations for candidate conformers. Combining spectroscopic and energetic results establishes that the metal ion is always chelated by the amide carbonyl oxygen, whilst the C-terminal hydroxyl does not complex the metal ion and is in the endo conformation. It is also likely that the aromatic ring of Phe always chelates the metal ion in a cation-π binding configuration. Along with the amide CO and ring chelation sites, a third Lewis-basic group almost certainly chelates the metal ion, giving a threefold chelation geometry. This third site may be either the C-terminal carbonyl oxygen, or the N-terminal amino nitrogen. From the spectroscopic and computational evidence, a slight preference is given to the carbonyl group, in an RO_aO_t chelation pattern, but coordination by the amino group is almost equally likely (particularly for K^+PheAla) in an RO_aN_t chelation pattern, and either of these conformations, or a mixture of them, would be consistent with the present evidence. (R represents the π ring site, O_a the amide oxygen, O_t the terminal carbonyl oxygen, and N_t the terminal nitrogen.) The spectroscopic findings are in better agreement with the MPW1PW91 DFT functional calculations of the thermochemistry compared with the B3LYP functional, which seems to underestimate the importance of the cation–π interaction.

1. Introduction

Metal-ion complexation on the surface or in the interior of biomolecules is widespread in nature, providing the basis for a lively interest in modelling the underlying interactions in the gas phase. In the domain of peptide complexes, interest in such gas-phase models has led to extensive study of metal-ion amino-acid complexes, giving a detailed and precise understanding of the thermochemistry and structures of a number of systems.[1–11] Gas-phase studies of complexes involving much larger peptide substrates has become experimentally and computationally more accessible with the emergence of electrospray ionization and advances in computational tools. However, interpretation of results for large systems is not straightforward. A bottom-up approach is attractive to bridge the gap between small and large systems by progressing from amino acid monomers through dipeptides, and then on to larger oligopeptides, up to a limit where detailed understanding will inevitably be overwhelmed by the size and complexity of the systems. The present study follows this strategy in exploring dipeptide systems that can model cation–π interactions between peptides and alkali ions. The capability of cation–π complexation is provided by phenylalanine, which is the simplest amino acid having the possibility of a cation–π interaction in addition to the usual interactions of the ion with the Lewis-basic oxygens and nitrogens. The results for the two Phe-containing dipeptide substrates explored here, PheAla and AlaPhe, have many features in common with previous work on M^+Ala[12] and M^+Phe[7,8,13–16] complexes. The outstanding new feature introduced in progressing to the dipeptides is that the amide oxygen binding site appears for the first time, and turns out to be a dominant feature for complexation.

The thermochemistry and structures of the monomer complexes Na^+Ala, K^+Ala, Na^+Phe and K^+Phe have been investigated in numerous experimental and computational studies. Recently, the ability for the study of gas-phase complexes has been enhanced by the infrared (IR) spectroscopic capabilities achievable by coupling a mass spectrometer to a high-intensity broadly tunable IR light source. The new light sources making this possible include bench top OPO systems and larger-scale free-electron laser (FEL) facilities. Examples of

[a] *Prof. R. C. Dunbar*
Chemistry Department
Case Western Reserve University
Cleveland, Ohio 44106 (USA)
Fax: (+1) 216-368-3006
E-mail: rcd@po.cwru.edu

[b] *Prof. N. C. Polfer*[+]
Fritz-Haber-Intitute of the Max-Planck-Society
Faradayweg 4-6, 14195 Berlin (Germany)

[c] *Dr. J. Oomens*
FOM-Institute for Plasmaphysics Rijnhuizen
Edisonbaan 14, 3439 MN Nieuwegein (The Netherlands)

[+] *Current address:*
Chemistry Department
University of Florida, Gainesville, FL 32611 (USA)

[**] *IRMPD: Infrared multiple-photon dissociation.*

Supporting information for this article is available on the WWW under http://www.chemphyschem.org or from the author.

recent work on peptides include OPO laser studies,[9,17–19] and FEL studies using the FELIX (*f*ree *e*lectron *l*aser for *i*nfrared *e*xperiments) FEL[20] and the CLIO (*c*entre *l*aser *i*nfrarouge d'*O*rsay) FEL.[21] In these studies the IR spectrum of the complex is viewed in an "action spectroscopy" mode, in which the extent of IR multiple-photon dissociation (IRMPD) is plotted as a function of photon energy.

Numerous computational studies have appeared on complexes of amino acids, including Ala and Phe[8,13,22,23]. Experimentally, sodium and/or potassium ion complexes of both Ala[12] and Phe[16] have been characterized by IRMPD spectroscopy, and there are also examples of structural studies using this technique with other amino acid complexes.[1,9,24] The recent IRMPD spectroscopic study of M^+Trp complexes[25] is particularly helpful in the interpretation of complexes involving cation–π interactions, through the characterization of the mixtures of conformers present in the Trp systems.

Experimental Section

IR Spectroscopy

The experimental apparatus,[26,27] methods and protocols are similar to previous work with alkali complexes of amino acids.[25] Solutions of 1 mM dipeptide with 1 mM MCl (where M = Na or K) were made up in 80% MeOH and 20% H2O. The metal cation–dipeptide complexes were generated by electrospray ionization (ESI) and accumulated with collisional cooling for 1–2 s in a hexapole, following which they were transferred to the Penning trap of the Fourier transform ion cyclotron resonance (FT-ICR) mass spectrometer. Ions were captured in the Penning trap with minimal collisional excitation by a field-switching approach in the transfer octopole.[7] The ion of interest was mass isolated and then irradiated with 10 macropulses from the FELIX laser to induce IR multiple photon dissociation (IRMPD).

While the IRMPD spectrum is not identical to a linear absorption spectrum, the assumption that the IRMPD yield is linearly proportional to the IR absorption intensity has been considered to be a useful approximation,[28] making it possible to view the IRMPD spectrum as a reflection of the true IR absorption spectrum. For the K^+ complexes, the photofragment ion was K^+. For the Na^+ complexes, some Na^+ was observed, but in addition, a major dissociation channel was observed at m/z 188, a loss of 71. The nature of this rearrangement fragmentation process was not clarified. No marked difference in the IRMPD spectra of the two channels of the sodium ion complexes is observed, and their intensities are summed.

Conformation Labeling

The chelation patterns discussed here are specified by a uniform labeling format. The five identifiable binding sites are the π-ring system (R), the amide oxygen (O_a), the carboxyl carbonyl oxygen (O_t), the hydroxyl oxygen (OH), and the N-terminal nitrogen (N_t). For labeling the ring-chelated complexes, we have encoded their arrangement using a conventional ordering of the ligands, by placing the metal above the ring, looking down on the complex, and ordering the ligands counter-clockwise. In the non-ring-chelated structures, our encoding scheme indicates the identities but not the arrangement of the chelating ligands. In presenting specific examples of the various conformations, we have also used a systematic letter classification of the chelation patterns (without regard to the order of the ligands) as follows: A for RO_aO_t; B for RO_aN_t; C for O_aO_t; D for $O_aN_tO_t$; E for four-fold chelation; F for RO_aOH; G for RN_tOH; H for RO_tN_t. Finally, an asterisk is appended when the carboxyl OH is in the *exo* conformation. Thus, for example, the conformation of K^+PheAla would be [KFA A4* RO_aO_t], whose structure appears in Figure S4 of the Supporting Information.

Choice of DFT Functional

The B3LYP functional has been widely used, and is generally considered satisfactory for alkali–ion complexes. Two alternatives are noteworthy. The BP86 functional has been recommended as giving slightly more accurate absolute binding energies for Na^+ complexes,[33] but generally it is found that it gives results quite similar to B3LYP in most respects. It has not been suggested as being superior in terms of cation–π binding energetics, and so was not used here. For complexes involving transition metals binding to aromatic ligands, it has been suggested that the MPW1PW91 functional is more accurate than B3LYP in the energetic comparision of π-binding sites with other types of sites, and specifically that B3LYP underestimates the strength of π-ring binding.[29,30] Such an advantage for MPW1PW91 has not been suggested for alkali metal-ion complexes, but it was decided to try it in this context, and accordingly the thermochemistry was calculated using both functionals for comparison. As described below, the comparison of functionals showed a small but significant difference in the description of the ring chelation energy, and there was some indication that MPW1PW91 was more accurate. Accordingly, all of the thermochemical considerations were approached using MPW1PW91 enthalpies, while the spectra were calculated using B3LYP for consistency with previous work on similar systems. Spectra calculated with MPW1PW91 were found to differ only very slightly from those obtained using B3LYP.

Conformation Searching and Energy Calculations

The conformation space of the complexes was quite widely searched, although no fully satisfactory, comprehensive search method was found. It is expected that all of the good candidates for the ground state of each complex are located, and that representatives of the most stable conformational patterns are found.

Initial searches were Molecular Mechanics (MM) surveys using the Amber99 force field (implemented in the HyperChem 7.5 search engine). Utilising a usage-directed variation of initial conformations, about 1000 initial structures seemed to be sufficient to locate all the good conformations, yielding about 300 candidate structures within 20 kJ mol^{-1} of the most stable one, including duplicates. After eliminating the obvious duplicates, the candidates were refined at the level of HF/STO-3G. However, the Amber force field was not found to be very satisfactory for these cation–π chelating systems, with numerous reasonable structures being missed in these searches. Additional searches were made directly using HF/STO-3G calculations for energy screening at the 20 kJ mol^{-1} cutoff level, which uncovered additional candidate structures. This direct HF searching was expensive, and only about a hundred trial geometries were calculated for each complex, which was insufficient to ensure full coverage of the conformation space. As a third approach, it was hoped that a semiempirical HF method might provide sufficiently accurate energies for comprehensive conformation searching in a reasonable time, but the common semiempirical parametrizations (AM1, PM3, ZINDO) were found to give poor

energetics and structures for these cation–π systems, and no useful results.

The combined sets of conformations obtained from the MM and HF searches were refined with the higher level DFT calculations, resulting in the sets of low-energy conformations. All the energies were calculated with DFT/MPW1PW91, [6-31+G(d,p)]. For each complex, the three or four most stable conformations were compared using a larger basis, [6-311+G(2df,2pd)]. These larger basis calculations generally gave less than 1 kJ mol^{-1} change in relative energies compared with the lower-level DFT calculations, and did not affect the predictions of the ground states, so it was considered that the level of basis set was high enough that the accuracy was not basis-set limited. Thermal corrections to the enthalpies from 0 K to 298 K were made, but were less than 1 kJ mol^{-1}. BSSE corrections to DFT in systems similar to these are consistently found to be small and reasonably constant at the 6-31+G(d,p) level, and were not considered worth the effort of calculation for the purposes of the present study. In the DFT calculations of small model systems, a constant value of 4 kJ mol^{-1} was subtracted from all the raw DFT binding energies as a rough correction for BSSE, vibrational zero-point energies (ZPE), and thermal corrections from zero K to room temperature. The MP2 calculations were done with counterpoise BSSE corrections, and a constant value of 2 kJ mol^{-1} was subtracted to approximate the ZPE and thermal corrections.

Stabilities of the calculated complexes were assessed using free energy values, where the entropic contributions were assigned from the vibrational entropy corresponding to the calculated frequencies. Table 2 shows that the thermal and entropic corrections can affect the predicted relative stabilities of different conformers up to several kJ mol^{-1} in some cases. Full vibrational calculations at the DFT/B3LYP [6-31+G(d,p)] level were done on all the conformations considered to be possible candidates for the actual ground-state structures, as well as some other higher-energy structures having points of interest. All of the calculated DFT structures, and all of the vibrational calculations, are reported in the Supporting Information.

Assigning a precise scaling factor to the computed vibrational frequencies is somewhat uncertain. Some recent B3LYP calculations of systems involving amino acids and alkali ions have found best fits using factors of 0.960[16,31], 0.975[25], 0.98[8] and 0.987[32] using basis sets of varying sizes. The value of 0.960[16,31] seems low for the present protocol. The value of 0.975, assigned for Trp complexes using a larger basis than the present one,[25] is probably the most closely transferable to the present work. This value, which was observed to give as good fits as any to the spectra, was used throughout the present work. We have taken care not to make spectroscopic interpretations that are not robust within a range of scale factors from perhaps 0.960 to 0.985. All quantum calculations were performed using the Gaussian03W package.[33]

2. Results and Discussion

2.1 Model Systems and Chelation Expectations

The dipeptides are a useful transition between the well-studied binding chemistry of the isolated amino acids, and the study of metal-ion binding to oligopeptide and protein systems, which is less developed. These dipeptides, whilst simple enough for detailed structural investigation and computation, offer the full set of possible chelation sites for a metal ion occuring in larger oligopeptides containing Phe. A useful starting point can be a rough assessment of the relative binding strengths of the different sites available in the dipeptides constructed from Ala and Phe. We assume for the moment that there are no steric costs in achieving optimal chelation of the metal ion, and we ignore any hydrogen-bonding or other intramolecular interactions other than the direct interaction with the metal ion. One way to survey such idealized binding-site characteristics is via small model ligands displaying isolated binding sites. Although metal-ion affinities are experimentally known for some useful small model systems[34] they are often not consistently available or reliable. Therefore, rather than trying to use experimental values, we utilised a set of moderately good calculations on the following model set, which display the chemical environments present in these dipeptides, where the structures are chosen to contain well-defined single chelation points. Model calculations were chosen such that no major change of conformation or multiple chelation accompanied complexation. These systems also have roughly similar sizes in order to equalize polarization effects (Table 1). The model predictions are displayed pictorially in Figure 1.

Values calculated with the MPW1PW91/6-311+G(d,p) protocol are used in the following discussion, but it is of interest to compare this protocol with the MP2 protocol used by Hoyau et al. [MP2/6-311+G(2d,2p)//MP2/6-31G*] in their survey of Na^+ affinities. Both sets of values are given in Table 1. The DFT and MP2 protocols yield quite similar results for the K^+ complexes, while the differences for the Na^+ complexes are larger

Table 1. Metal-ion bond dissociation energies of small model compounds containing the five Lewis-basic chelation sites for the dipeptides. Values [kJ mol^{-1}] calculated at the DFT MPW1PW91/6-311+G(d,p) level. For comparison, values [kJ mol^{-1}] are also given using an MP2 protocol [MP2/6-311+g(2d,2p)//MP2/6-31g*] with approximate corrections for 298 K thermal effects, BSSE and zero-point energies.

Type of site	Model compound	Na^+		K^+	
		DFT	MP2	DFT	MP2
Amide C=O (O_a)	N-methylacetamide	165	154	125	123
Acid C=O (O_t)	Acetic acid	118	108	84	83
Ring (R)	Benzene	99	88	69	72
Terminal N (N_t)	Aminoacetone	96	90	61	63
Acid OH (OH)	Acetic acid	55	53	31	35

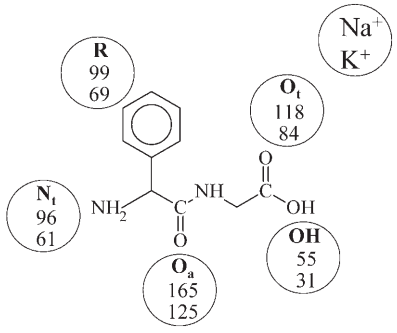

Figure 1. Calculated metal-ion affinities of dipeptide binding sites (kJ mol^{-1}) derived from calculations of simple model systems (Table 1) using DFT MPW1PW91/6-311+G(d,p) for Na^+ (top row) and K^+ (lower row).

(up to 11 kJ mol^{-1}). Similar to the results observed by Armentrout and Rodgers for the B3LYP functional, our DFT calculations for the sodium ion complex are both a few kJ mol^{-1} higher and also somewhat scattered compared to those obtained with MP2.[35] (They found that either MP2 or DFT/B3P86 gave better results for Na^+; however, all of these methods give results that are adequate for the present purposes). No conclusion seems warranted about the accuracy of the calculations for K^+ complexes. The observations and conclusions given later about the binding sites are equally valid using either DFT or MP2 binding energies.

The models indicate that the amide oxygen site (O_a) is highly favoured and should be consistently metalated. It is thus not surprising that the calculations of Wang et al. found that polyglycines and polyalanines as large as the tetrapeptides, commonly favour chelation by all the available CO groups prior to populating the N_t binding site.[36] However, it is slightly surprising that for tetra-alanine, where two approximately equal lowest-energy conformations are observed, one of these conformations has one of the three O_a sites unchelated while the O_t site is chelated. For various dipeptides where calculations have been reported,[36–43] the O_a site is always chelated in the low-energy conformers, as expected.

The terminal carboxyl C=O (O_t) is favoured over the remaining sites. The ring (R) is not very different from the NH_2 site (N_t) in binding affinity, and these two sites should be competitive, although the MPW1PW91 results indicate a small preference for the ring over the NH_2. The hydroxyl site (OH) is much less favoured, and should not be a competitive binding site. The amide nitrogen does not offer a favourable chelation site; attempts to model a metal ion near this nitrogen resulted in spontaneous migration of the metal to the nearby oxygen. It should be stressed that these intrinsic relative site affinities are only a starting point, and the relative stabilities of actual conformers of peptide complexes having various chelation patterns can be drastically altered by steric strain, intramolecular H-bonding, and other perturbations.

Moision and Armentrout have applied a similar approach to analyzing metal-ion (Na^+ and K^+) complexes with glycine,[44,45] in which a set of single-site and bidentate model ligands was used to generate single-site metal-ion affinities. They achieve detailed dissections of various factors acting to determine the structures of the complexes. Their studies are not easily compared with the present work, because they used a different set of model complexes not well suited to dipeptide modelling. Their modelling scheme suggests that Na^+ has a significant enhancement in the relative affinity of the nitrogen site compared with K^+, which was considered to be responsible for the systematic Na^+/K^+ differences in the stabilities of various chelation patterns. However, our model does not suggest a similar effect, nor did our calculated comparisons of chelation schemes show any obvious favouring of nitrogen chelation for Na^+.

The sodium complexes of GlyHis and HisGly have been studied computationally,[39] and may provide interesting parallels to the present results, since the His side-chain can function as a π-chelating ligand, although edge-chelation of the metal ion by one of the ring nitrogens is more favourable when sterically feasible. Thus the N^{ε}–H tautomer of both isomers, in which edge-on interaction of Na^+ with the imidazole ring is possible, provides the most stable conformations. In the N^{δ}–H tautomers, where an edge-on interaction is not possible, the imidazole ring gives cation–π chelated conformations, but their stability is lower by ~40 kJ mol^{-1} than the best N^{ε}–H structures.

The IRMPD spectra are shown in Figure 2. The experimental spectra are accompanied by computed spectra representing either the most stable conformation, or a mixture of low-energy conformations, illustrating one out of many possible mixed populations giving acceptable fits to the observed spectrum. The quality of the spectra is sufficient for a detailed consideration of the structures of the complexes. A useful starting point is the comparison of the four spectra, which are seen to be very similar in the number, positions and intensities of the major peaks. The close similarity of the spectra obtained from the four systems might indicate that the chelation pattern is the same. The close correlation of the spectra with the calculated structures indicates that the most favoured structural motif has threefold chelation, RO_aO_t or RO_tO_a, with the metal ion being chelated by the ring and the two carbonyl oxygen atoms. If one were forced to choose a single chelation pattern, this would be the most attractive. However, the three-fold chelation, RO_aN_t or RN_tO_a, involving the amide oxygen, the ring, and the terminal nitrogen is almost as good, and may well make up part of the ion populations. Conformations in which the ring is not chelated are less attractive, yet detailed examination shows that some contribution from such structures also cannot be ruled out. Overall, the agreement of the observed spectra with the computational expectations is satisfactory.

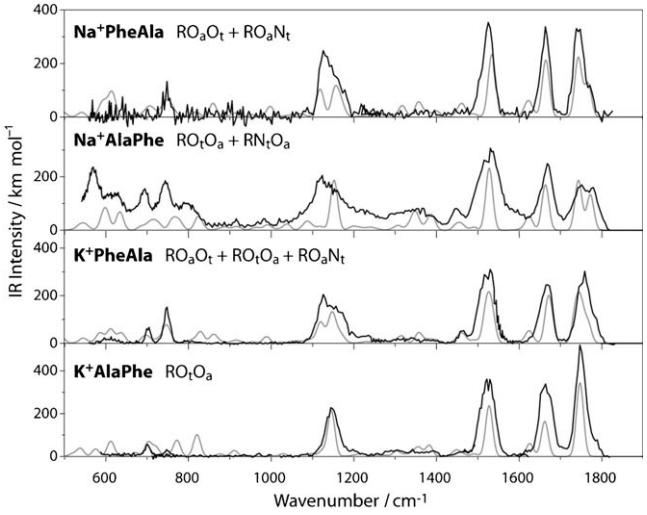

Figure 2. IRMPD spectra of the four complexes (black lines) along with the calculated spectrum of the most stable conformer, or of a mixture of conformers of similar stability (grey lines). For a mixture, the theoretical spectra of the relevant conformers are simply co-added.

2.2 Structural Interpretations

There are hundreds of possible conformations of each of these complexes, many of which are stable local minima on the potential energy surface. In order to narrow these down and draw structural conclusions, it is necessary to compare the spectra with the calculated spectra for the energetically reasonable possibilities. This enables the assignment of one or several conformations that make up the population of ions in the trap. The structure search methods used were not exhaustive, but were sufficiently broad to locate all of the conformations lying within a few kJ mol^{-1} of the most stable one, and therefore can be used to identify the most probable chelation modes contributing to the populations. Figure 2 shows the fits obtained from the lowest energy conformer, or a mixture of conformers of similarly low energy, for each of the four spectra.

Within the large number of conformations found by broad searching procedures, we carried out high-level optimization and energy calculations on those that seemed most likely to be close to the ground state, also including representative examples of other reasonably favorable chelation patterns. The set of example conformations is shown in Table 2. Figures 3 and 4 show representatives of the various chelation patterns calculated, and the actual structures of all the conformations are provided in Figures S1–S4 of the Supporting Information. As indicated in Table 2, many of the chelation patterns give multiple low-energy conformations in our searches, and in addition, many other conformations exist but are not considered likely to be stable enough to warrant high-level calculation.

Table 2. Calculated thermochemistry of low-energy complex conformations. Values [kJ mol^{-1}] are given in the form [Na^+ complex]/[K^+ complex]. Calculations are DFT/MPW1PW91 except for the last column, which is DFT/B3LYP.

	Chelation	ΔH 0 K	ΔG 298 K	ΔG B3LYP
M^+PheAla				
A1	RO_aO_t	0/0	0/0	0/0
B1	RO_aN_t	7/4	3/2	4/4
A2	RO_tO_a	8/2	6/0	7/1
C1	O_aO_t	16/7	7/1	4/−4
A3	RO_tO_a	16/	13/	13/
D1	$O_aO_tN_t$	20/13	17/11	17/12
D2	$O_aO_tN_t$	/18	/15	/13
A2*	RO_tO_a*	/19	/17	/19
E1	$RO_tO_aN_t$	23/9	22/9	24/12
A1*	RO_aO_t*	23/19	21/17	22/19
E2	$RO_tO_aN_t$	28/	26/	27/
C2	O_aO_t	38/27	34/15	28/13
F1	RO_aOH	42/34	39/33	41/33
M^+AlaPhe				
A1	RO_tO_a	0/0	0/0	0/0
B1	RN_tO_a	4/9	6/10	5/5
D1	$O_aO_tN_t$	21/23	22/23	19/14
D1*	$O_aO_tN_t$*	18/19	19/18	18/16
C1	O_aO_t	18/15	15/12	11/3
C1*	O_aO_t*	18/13	15/10	15/6
B2	RO_tN_t	24/27	26/30	27/27
A2	RO_tO_a	29/28	28/29	27/25
F1	RO_aOH	28/28	29/34	30/32
B3	RO_tN_t	/34	/38	/39
B4	RO_aN_t	/40	/43	/36
G1	RN_tOH	/59	/63	/60

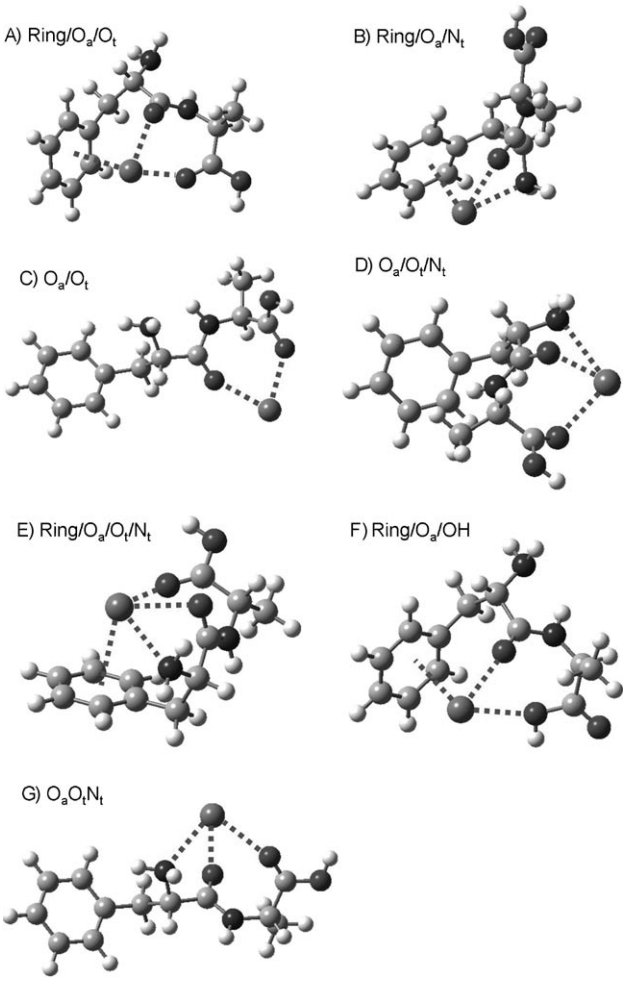

Figure 3. Computed favorable chelation patterns for the M^+PheAla complexes.

2.3 Zwitterion Possibilities

It has been well established that the IR spectra of metal-ion complexes of amino acids provide a clear distinction between the zwitterion (or salt bridge) tautomer and the neutral (or charge solvation) tautomer of the amino acid. The zwitterion form is distinguished by a strong CO_2^- band between 1650 and 1700 cm^{-1} as well as a strong NH_3^+ band around 1400 cm^{-1}, while the neutral form gives a strong characteristic C=O stretching band between 1700 and 1775 cm^{-1}. The present spectra show the signature C=O band at about 1750 cm^{-1} that is diagnostic for the neutral form of the terminal COOH group. The absence of any feature in the 1400 cm^{-1} region indicates a lack of appreciable zwitterion contributions. No conclusion about the possible presence of zwitterion component can be drawn from the presence of the band at 1675 cm^{-1}, since this is also the position of the strong amide N–H bend that is expected in any case for the dipeptides.

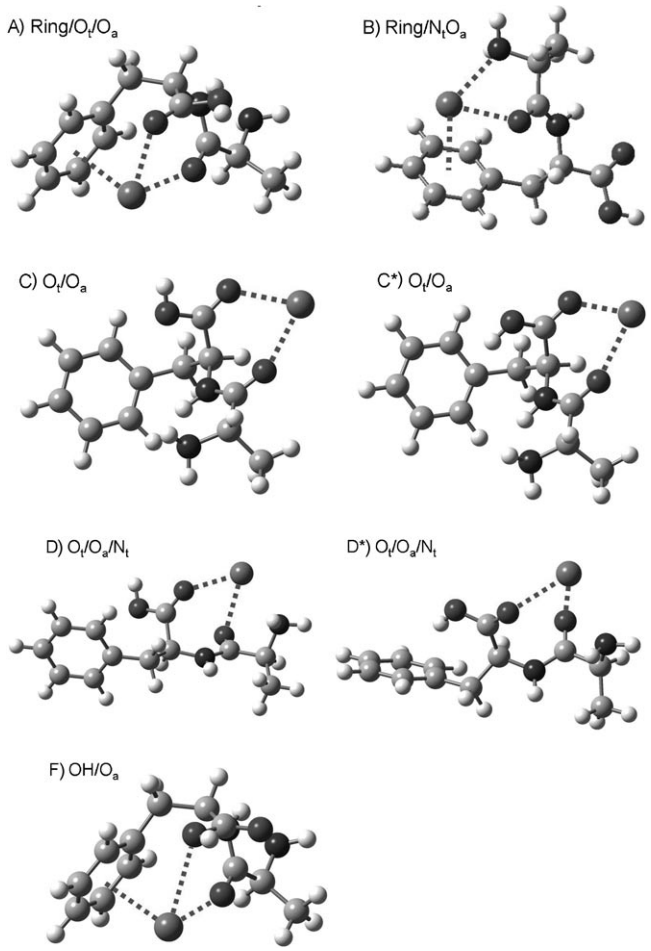

Figure 4. Computed favorable chelation patterns for the M^+AlaPhe complexes.

Computationally, no zwitterion structures were found with energies competitive with the favorable charge-solvated isomers. The best configuration for zwitterion stability is commonly found to be a salt-bridge geometry in which the negative charge of the CO_2^- is stabilized by proximity to the positive NH_3^+ group as well as the metal ion. Trial zwitterion structures of this type rearranged spontaneously to the neutral form by proton migration from NH_3^+ to CO_2^-. Since the spectra conclusively rule out predominant zwitterion structures, and such structures have not been found to be energetically competitive in gas-phase metal-ion complexes with either Ala or Phe monomers, we did not pursue computational investigation of other zwitterion structures.

2.4 Configuration of Carboxyl OH

The interaction of the hydroxyl with the neighbouring carbonyl oxygen is around 20 kJ mol^{-1}, as shown by the comparison of the *endo* (interacting) and *exo* (non-interacting) conformations as shown in the examples of K^+PheAla A1 versus A1*; K^+PheAla A2 versus A2*; Na^+PheAla A1 versus A1*. These examples with PheAla complexes assess the interaction strength by comparison with the non-interacting forms where the hydrogen has no intramolecular hydrogen bond. A similar *endo* interaction strength would be anticipated for AlaPhe complexes in the absence of hydrogen bonding. However, with the AlaPhe complexes, the most interesting and most stable *exo* configurations are those which are able to form an OH···π-ring hydrogen bond, which compensates the loss of the OH···OC interaction in the *endo* configuration. This OH···π-ring is sufficiently strong so that the *exo* and *endo* conformations are not very different in stability (suggesting an OH···π stabilization also of the order of 20 kJ mol^{-1} as in KAlaPhe C1 versus C1*; KAlaPhe D1 versus D1*; NaAlaPhe D1 versus D1*). Such XH···π hydrogen bonds are well known structural features of peptides.[46] The spectral signature of the *exo* conformation of the OH is the shift of the OH bend from ~1150 cm^{-1} (*endo*) to ~1250 cm^{-1} (*exo*). The experimental spectra obtained (Figure 2) show a strong feature at ~1150 cm^{-1}, and no significant peak around 1250 cm^{-1}, clearly indicating the *endo* conformation in all cases.

2.5 Extent and Nature of Chelation

Complex conformations of reasonable stability were found with two-fold (C), three-fold (A, B, D, F and G) and four-fold (E) chelation of the metal ion (see Table 2, Figures 3 and 4 and Figures S1–S4 for examples). Table 2 indicates that three-fold chelation gives the most stable conformations in each case. However, two-fold chelation is able to give nearly equally stable complexes (with respect to relative ΔGs) for K^+ complexes (as in K^+AlaPhe C1 and K^+PheAla C1). The fourfold chelated conformations that we located were all substantially less stable than the best structures.

The two-fold chelated conformations without ring chelation (chelation type C) are extended, loose structures with relatively high entropies, as reflected by the fact that their relative free energies (Table 2) are more favourable than their relative enthalpies. Thus the greater conformational flexibility of the two-fold chelation pattern can compensate partially for their generally less favourable chelation enthalpy, compared with the three-fold chelated forms, although this compensation is never large enough to allow any of them to be the overall ground state conformation. Surprisingly, the relative entropies of the threefold and fourfold chelated conformations were not very different. We surmise that the steric strain and bond misalignment accompanying the achievement of any of the fourfold chelated conformations results in bond loosening, which counteracts the tightening effect of the more constrained fourfold chelated geometries and gives a net similarity of entropies.

As expected from the small-molecule models, all conformations of reasonable stability include O_a chelation. Moreover, the most stable conformations in each case are achieved by chelation of the three ligands predicted by the small-molecule modelling to have the highest metal-ion affinities, namely O_a, O_t and R. However, Table 2 also indicates that conformations involving N_t chelation can be very competitive even though the model amino nitrogen has a somewhat lower metal-ion affinity than the other three types of isolated sites. Indicative of the limitation of the small-molecule models, the high stability

of the B1 conformations (RO_aN_t) is unexpected from the models, which would suggest that O_t would always chelate in preference to both R and N_t. As predicted from the models, OH chelation is not thermodynamically competitive, and the most stable conformations involving this ligand that we found, as indicated in the table, are substantially less stable than the overall best conformations. Thus the model-derived predictions of exceptionally strong chelation by O_a, and exceptionally weak chelation by OH, are found by experiment and by computations to be dominant effects; while the other three chelation sites, O_t, N_t and R, can all be competitive chelators, depending on details of steric strain and other secondary intramolecular interactions.

2.6 Predicted Versus Observed Spectra

Out of the conformers located in the low-level searches, higher-level DFT calculations were done on those that seem likely to have competitively high stabilities, as well as some less stable conformers of particular interest (Table 2). The predicted IR spectra of many of these are plotted in Figures 5 to 8, with additional spectra provided in Figures S5 to S8 of the Supporting Information.

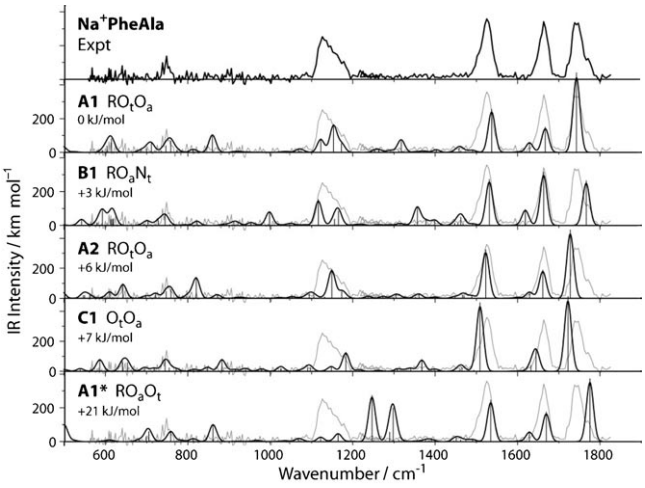

Figure 5. Experimental spectra (top panel and grey lines in subsequent panels) and low-energy conformations (black lines) of Na^+PheAla. (The asterisk, as in the label of the bottom spectrum, indicates the *exo* configuration of the carboxyl OH.)

Many of the predicted spectral features correspond to vibrational types that are common across all four systems. These recurrent normal modes are described on the calculated A1 spectrum of K^+PheAla in Figure 6.

One general feature is that all calculations predict a feature of varying intensity near 1620 cm^{-1} corresponding to the NH_2 scissoring vibration. Except for the suggestion of a possible small shoulder in the spectrum of the K^+AlaPhe complex, none of the observed spectra show a discernable peak above the background noise in this vicinity. Evidently, this vibration is

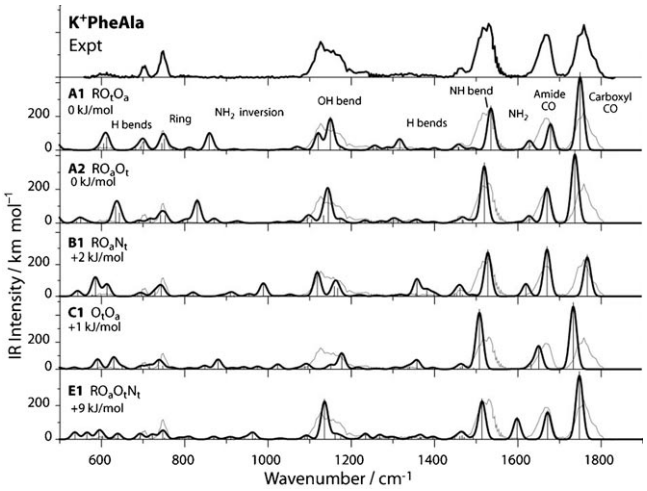

Figure 6. Experimental spectrum (top panel and grey lines in subsequent panels) and low-energy conformations (black lines) of K^+PheAla.

rather weak for all four systems, which provides an argument against many possible structure assignments for which this feature is predicted to be strong. Another frequent feature in the calculations is a peak corresponding to the NH_2 inversion mode of the NH_2 group (or the frustrated inversion, in situations where the nitrogen is metal-ion chelated). This mode is predicted with reasonable intensity by harmonic force-field calculations anywhere from 800 to 1100 cm^{-1} (for example, at 860 cm^{-1} in Figure 6, A1). Such a peak is not apparent in most of the observed spectra. This mode is thought to be highly anharmonic, and strongly variable in predicted frequency depending on the chelation situation of the terminal nitrogen. In general, it is not expected to be well treated by the harmonic vibrational calculations at the present level of theory. Thus the non-appearance of such a peak at the calculated position in the spectra has not been considered as a significant counter-indication of a fit.

It had been hoped that the peaks observed in the 550–800 cm^{-1} region of the spectrum would provide key diagnostic structure indicators, since ring out-of-plane H-bending modes appear in this region, and might be expected to be strong indicators of the state of ring chelation. This hope was generally not borne out. The calculated peaks in this region are generally quite weak, and reliable correlations of distinctive predicted peaks with particular patterns of ring chelation did not emerge. Thus, no obviously useful information could be ascribed to the rather weak experimental peaks in this region. The best-fit conformational patterns usually provide acceptable fits to the spectra in this region, yet many other conformations also give sufficiently good fits.

Further conclusions from the spectroscopy depend on a more detailed look at the spectra for the different dipeptide/metal combinations, which, while similar, are not exactly identical.

2.7 M^+PheAla

The Na^+ and K^+ complexes of PheAla gave virtually indistinguishable spectra, suggesting similar conformations. Calculated spectra of chelation types A, B and C all have low enough free energies to be believable candidates, and all give not-too-bad fits to the spectra, so they all need to be carefully considered before drawing conclusions. In particular, the lowest four conformations found for K^+PheAla have computationally identical free energies within reasonable uncertainty. For Na^+PheAla, the A1 conformation has a more significant calculated free-energy advantage over the other three low-energy conformations, but the differences are still small.

The non-ring chelated structures (types C and D) are spectroscopically less satisfactory than the A and B types. Four examples of type C and two of type D are given in Figures 5 and 6 and Figures S5 and S6 of the Supporting Information. The most convincing argument against the C structures is the fact that the calculations give a small peak at 1130 cm^{-1}, which is the location of the observed maximum of the broad experimental peak in this region. The predicted position of the OH bending peak in the C structures is around 1180 cm^{-1}, which is not very close to the peak of the observed feature; and additionally the calculations of all four C spectra give the carboxyl CO peak about 30 cm^{-1} to the red of the observed peaks. The two conformations with structure C2 are further disfavored in that a strong peak is predicted, but not observed, for the NH_2 scissoring vibration at 1600 cm^{-1}. However, this last argument does not rule out the C chelation type in general, because the NH_2 scissor is calculated to be very weak for the C1 structures. Furthermore the peaks near 1500 and 1670 cm^{-1} are calculated at noticeably lower frequencies than observed. Finally, examples are shown (D1 in Figures S5 and S6 of the Supporting Information) of non-ring-chelated conformations with threefold chelation. These do not give a very good match to the observed spectra, particularly with respect to the predicted peak at 1600 cm^{-1}, and this, along with the fact that no such conformations were found with free energies competitive with the ring-chelated conformations, makes the D chelation type unattractive. In summary, the non-ring-chelated geometries give quite poor agreement with the observed spectra. The C2 and D1 structures are probably not important, based on both energetic and spectroscopic arguments, and the C1 structure, while energetically feasible, is far enough from a good spectroscopic fit to make it unlikely as a major contributor, although some contribution from C1 cannot be ruled out.

The ring-chelated conformations of type B1 shown in Figures 5 and 6 (ring, amide oxygen and terminal NH_2) are stronger contenders. Energetically, they are not far from chelation type A, and spectroscopically they match quite well. The calculated carboxyl CO stretch near 1750 cm^{-1} is slightly to the blue compared with type A chelation. It is possible, in the spectra of both metal-ion complexes, to match this predicted peak with a possible shoulder near 1780 cm^{-1} for both metals, which would be consistent with a mixture of A1 and B1 conformations. The B1 calculations actually give a better fit than type A to the broad feature around 1150 cm^{-1}. (The good fit to this feature is due to a strong mode at 1120 cm^{-1} of largely H-bending character in the B1 structures that has no counterpart in the A structures.) Arguing against a predominance of the B structure type is the prediction for these structures of a strong H-bending mode at 1350 cm^{-1} which is not observed in the spectra. In other respects, the B1 structure fits the spectra about as well as the A1 structures. We thus consider it quite possible that the B1 structures contribute importantly to the ion populations, which could be a nearly equal mixture of A1 and B1 conformations. The "best match" simulated spectrum in Figure 2 for K^+PheAla is an equal mixture of structures A1, A2 and B1, and gives a satisfactory fit, although other combinations of the low-energy conformations are just about as good. Similarly, the "best match" in Figure 2 for Na^+PheAla is an equal mixture of A1 and B1, although other combinations are also reasonable.

2.8 M^+AlaPhe

The A1 conformation has a significant free energy advantage for the AlaPhe complexes, (see Figures 7 and 8) although the B1 conformation is also energetically feasible for both metals, and non-ring-chelated C1 conformation are also not too unfavorable. The most stable calculated A1 conformations agree well with the K^+AlaPhe spectrum, and not quite as well with the Na^+AlaPhe spectrum.

For Na^+AlaPhe, (Figure 7) the B1 conformation also gives an acceptable match, and a combination of A1 and B1 gives a nice correspondence with the apparent splitting of the C=O stretching feature around 1750 cm^{-1} in the experimental spectrum. Thus the "best match" in Figure 2 is suggested as an equal mixture of A1 and B1.

For K^+AlaPhe (Figure 8) no calculated conformation other than A1 agrees with all of the observed peaks, and it is concluded from the spectrum that A1 is the only important chelation mode. The B1, C1 and C1* conformations all have fairly good stability, but none of them gives a very good fit to the spectrum. The D1 conformation shows somewhat better

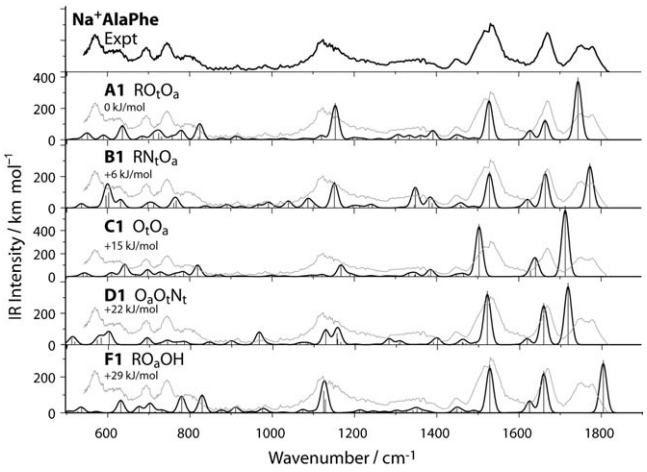

Figure 7. Experimental spectrum (top panel and grey lines in subsequent panels) and low-energy conformations (black lines) of Na^+AlaPhe.

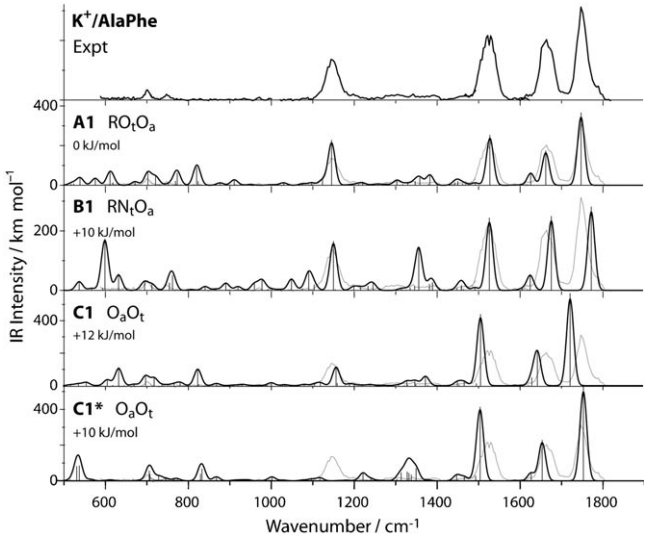

Figure 8. Experimental spectrum (top panel and grey lines in subsequent panels) and low-energy conformations (black lines) of K^+AlaPhe.

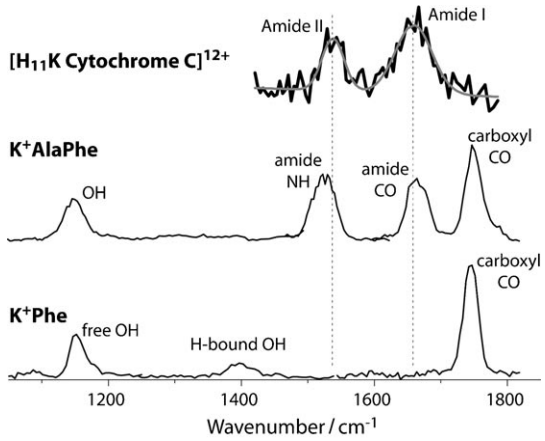

Figure 9. Comparison of the IRMPD spectra of the K^+ complexes of Phe and AlaPhe, and the 12^+ protonated charge state of cytochrome-C.

agreement with the spectrum, but at $+23\,kJ\,mol^{-1}$ relative free energy, it is probably not sufficently stable to be a serious possibility. Thus the "best match" for this spectrum in Figure 2 is assigned as pure A1.

2.9 Other Chelation Possibilities

Fourfold chelated conformations of the complexes were found as minima on the potential energy surfaces, but none were found having stability competitive with the various low-energy two-fold or three-fold chelation patterns discussed above. A typical example of such a conformation for Na^+PheAla is NaFA E1 $RO_tO_aN_t$, whose structure and calculated spectrum are shown in Figs. S1 and S5 of the Supporting Information, respectively. The calculated spectrum is actually not bad (except for a too-intense predicted NH_2 peak at 1590 cm−1), but it is calculated to be disfavored by 22 $kJ\,mol^{-1}$ in free energy.

2.10 Comparisons

The dipeptide spectra allow us to view the spectroscopic evolution from amino acid complexes to peptides, as shown in Figure 9. The spectrum of K^+Phe was reported previously,[16] but its quality was poor, and the improved ion cooling in the current configuration of the instrument[7] generates the new, much improved spectrum displayed. Also shown in Figure 9 is the spectrum reported for the $+12$ charge state of potassiated protonated bovine cytochrome C.

Comparing the K^+Phe and K^+PheAla spectra, we see the appearance of the characteristic amide bands in the dipeptide spectrum. Amide I (C=O stretch) and Amide II (N–H bend) are in blank regions of the K^+Phe spectrum. Both spectra show the strong peak for the terminal carboxyl CO group, and a strong peak for the carboxyl OH group not H-bound to the NH_2 group. The K^+Phe spectrum also shows a peak at 1400 cm^{-1} corresponding to conformations where the OH group is hydrogen-bonded to the NH_2 group. No such peak is predicted for the dipeptide, since it is found to be sterically impractical to form low-energy conformations having such a hydrogen bond in this case. In both monomer and dipeptide cases a peak is predicted near 1600 cm^{-1} for the NH_2 scissors vibration, but its predicted intensity is low; being barely discernible in the monomer case, and not seen at all in the dipeptide case.

The cytochrome C spectrum was acquired only over a more limited wavelength region, but it clearly shows the Amide I and Amide II bands. In the protein, the position of the Amide I band is red-shifted relative to the dipeptide, whereas the Amide II band is blue-shifted, as would be expected for increased hydrogen bonding interactions. Interestingly, the peak widths of both bands are comparable in both the dipeptide and protein. In the spectrum of the protein no peak is visible for the carboxylic acid CO stretching vibration. The disappearance of this peak is expected, since there is only a single terminal carboxylic acid, whereas there are over a hundred amide CO groups (103, to be exact). Therefore, even if this carboxylic acid is not deprotonated, as it may be in the protein, its characteristic peak will be insignificant relative to the strong amide peaks. Thus the dipeptide spectrum represents a graphic transition from the monomer complex to the protein, showing recognizable bands corresponding both to the terminal carboxyl group that plays a prominent role in the monomer complex spectrum, and also to the amide linkage that dominates the spectroscopy of large peptides.

2.11 Comparison of DFT Functionals

There was a significant difference in the treatment of ring chelation by the B3LYP functional versus the MPW1PW91 functional. In this study, 38 dipeptide complex conformations were calculated using both functionals. Over this sample, MPW1PW91 was found to favor ring-bound conformations more strongly than B3LYP by 3 $kJ\,mol^{-1}$.

It is not known a priori which functional is more accurate in treating the cation–π interaction. The present results give

some experimental evidence on this question. There is one case where the functionals make opposite predictions about the ground state, which is K^+PheAla, where a non-ring-bound structure (C1, O_tO_a) was calculated by B3LYP to be the most stable structure by several kJ mol^{-1}, while MPW1PW91 gives two ring-chelated structures with greater stability than this one. The spectroscopic result is in favor of the MPW1PW91 predictions, in that both of the structures predicted to be most stable are excellent fits to the observed spectrum, while the (C1, O_tO_a) structure is a poor fit. This is another piece of evidence to add to previous indications[29,30] that MPW1PW91 is superior in its thermochemical treatment of ring-chelated complexes. Accordingly, we adopted MPW1PW91 values for the thermochemical comparisons here. However, we have retained the B3LYP results for vibrational properties and spectral predictions, to provide more direct comparison with other laboratories' computations, and because there is no indication of superiority of MPW1PW91 for vibrational properties.[31]

3. Conclusions

The combination of computational results and spectroscopic observations gives a number of structural conclusions about these dipeptide complexes. Firm conclusions are that there are no zwitterionic conformations in the populations, and that the terminal OH group of the C-terminus is exclusively in the *endo* conformation. Among the five available Lewis-basic chelation sites, it is clear that the amide CO group always chelates the metal ion, and the terminal OH group does not do so. This is also consistent with previous computational results on the potassiated pentapeptides Leu-enkepahlin and bradykinin, where the peptides were found to be wrapped around the metal cation, maximizing the electrostatic interactions with the carbonyl oxygens.[16]

Among the remaining three possible sites, there are possibilities for various chelation combinations. The spectroscopic evidence indicates that the ring always provides one chelation site in a cation-π binding mode. For the Na^+ complexes the metal-ion/ring interaction is strong enough so that non-ring-chelated conformations were found to be energetically uncompetitive, reinforcing the spectroscopic evidence. For the K^+ complexes, non-ring-chelated complexes were located having nearly competitive energies, but it was considered that the spectroscopic arguments in favor of ring chelation were strong in all cases. It is notable that thermochemical calculations with the MPW1PW91 functional were in better accord with the relatively high favorability of the ring binding site than the B3LYP functional, and the latter functional was considered to be less satisfactory than the former for modeling this aspect of metal-ion binding for sodium and potassium ions.

Having established the amide CO and the ring as two chelation sites, we found that there is definitely a third metal chelation at one of the terminal sites, either the terminal CO group, or the terminal NH_2 group. In general, conformations with either of these chelation patterns were acceptable on both energetic and spectroscopic grounds, and it seemed likely that the populations were mixtures of the two types. Only for K^+ AlaPhe was there a clear preference for one of the possibilities, namely A-type chelation at the O_t site.

The gas-phase spectroscopy of the dipeptide complexes was found to give a nice transition between the spectrum of the monomeric Trp complex and the cytochrome-C spectrum. The monomer complex is dominated by vibrations associated with the N-terminal and C-terminal groups, while the cytochrome-C spectrum is dominated by amide bands. The dipeptide complexes show vibrational features corresponding to both of these types of vibrational modes.

Acknowledgements

This work is financially supported by the "Nederlandse Organisatie voor Wetenschappelijk Onderzoek" (NWO) and grant CHE-9909502 from the National High Magnetic Field Laboratory (Tallahassee, FL). R.C.D. acknowledges travel support from the National Science Foundation. The skillful assistance from the FELIX staff is gratefully acknowledged.

Keywords: alkali metals · density functional calculations · IR spectroscopy · mass spectrometry · peptides

[1] C. Kapota, J. Lemaire, P. Maître, G. Ohanessian, *J. Am. Chem. Soc.* **2004**, *126*, 1836–1842.
[2] T. Shoeib, K. W. M. Siu, A. C. Hopkinson, *J. Phys. Chem. A* **2002**, *106*, 6121–6128.
[3] T. Marino, N. Russo, M. Toscano, *J. Phys. Chem. B* **2003**, *107*, 2588–2594.
[4] R. A. Jockusch, W. D. Price, E. R. Williams, *J. Phys. Chem. A* **1999**, *103*, 9266.
[5] M. M. Kish, G. Ohanessian, C. Wesdemiotis, *Int. J. Mass Spectrom.* **2003**, *227*, 509–524.
[6] E. R. Talaty, B. A. Perera, A. L. Gallardo, J. M. Barr, M. J. Van Stipdonk, *J. Phys. Chem. A* **2001**, *105*, 8059.
[7] N. C. Polfer, J. Oomens, D. T. Moore, G. von Helden, G. Meijer, R. C. Dunbar, *J. Am. Chem. Soc.* **2006**, *128*, 517–525.
[8] C. H. Ruan, M. T. Rodgers, *J. Am. Chem. Soc.* **2004**, *126*, 14600–14610.
[9] M. F. Bush, J. T. O'Brien, J. S. Prell, R. J. Saykally, E. R. Williams, *J. Am. Chem. Soc.* **2007**, *129*, 1612–1622.
[10] M. T. Rodgers, P. B. Armentrout, *Acc. Chem. Res.* **2004**, *37*, 989–998.
[11] L. Operti, R. Rabezzana, *Mass Spectrom. Rev.* **2003**, *22*, 407–428.
[12] A. Simon, L. MacAleese, P. Maître, J. Lemaire, T. B. McMahon, *J. Am. Chem. Soc.* **2007**, *129*, 2829–2840.
[13] R. C. Dunbar, *J. Phys. Chem. A* **2000**, *104*, 8067–8074.
[14] V. Ryzhov, R. C. Dunbar, B. Cerda, C. Wesdemiotis, *J. Am. Soc. Mass. Spectrom.* **2000**, *11*, 1037–1046.
[15] A. Gapeev, R. C. Dunbar, *J. Am. Chem. Soc.* **2001**, *123*, 8360–8365.
[16] N. C. Polfer, B. Paizs, L. C. Snoek, I. Compagnon, S. Suhai, G. Meijer, G. Von Helden, J. Oomens, *J. Am. Chem. Soc.* **2005**, *127*, 8571–8579.
[17] H. Oh, K. Breuker, S. K. Sze, B. K. Carpenter, F. W. McLafferty, *Proc. Natl. Acad. Sci. USA* **2002**, *99*, 15863–15868.
[18] H. B. Oh, C. Lin, H. Y. Hwang, H. Zhai, K. Breuker, V. Zabrouskov, B. K. Carpenter, F. W. McLafferty, *J. Am. Chem. Soc.* **2005**, *127*, 4076–4083.
[19] A. Kamariotis, O. V. Boyarkin, S. R. Mercier, R. D. Beck, M. F. Bush, E. R. Williams, T. R. Rizzo, *J. Am. Chem. Soc.* **2006**, *128*, 905–916.
[20] J. Oomens, N. Polfer, D. T. Moore, L. van der Meer, A. G. Marshall, J. R. Eyler, G. Meijer, G. von Helden, *Phys. Chem. Chem. Phys.* **2005**, *7*, 1345–1348.
[21] B. Lucas, G. Gregoire, J. Lemaire, P. Maître, J.-M. Ortega, A. Rupenyan, B. Reimann, J. P. Schermann, C. Desfrancois, *Phys. Chem. Chem. Phys.* **2004**, *6*, 2659–2663.
[22] F. M. Siu, N. L. Ma, C. W. Tsang, *Chem. Eur. J.* **2004**, *10*, 1966–1976.
[23] J. M. Talley, B. A. Cerda, G. Ohanessian, C. Wesdemiotis, *Chem. Eur. J.* **2002**, *8*, 1377–1388.

[24] B. Lucas, G. Gregoire, J. Lemaire, P. Maître, J.-M. Ortega, A. Rupenyan, B. Reimann, J. P. Schermann, C. Desfrançois, *Phys. Chem. Chem. Phys.* **2004**, *6*, 2659–2663.
[25] N. C. Polfer, J. Oomens, R. C. Dunbar, *Phys. Chem. Chem. Phys.* **2006**, *8*, 2744–2751.
[26] D. Oepts, A. F. G. van der Meer, P. W. Amersfoort, *Infrared Phys. Technol.* **1995**, *36*, 297.
[27] J. Valle, J. R. Eyler, J. Oomens, D. T. Moore, A. F. G. van der Meer, G. von Helden, G. Meijer, C. L. Hendrickson, A. G. Marshall, G. T. Blakney, *Rev. Sci. Instrum.* **2005**, *76*, 023103.
[28] J. Oomens, A. G. G. M. Tielens, B. Sartakov, G. von Helden, G. Meijer, *Astrophys. J.* **2003**, *591*, 968–985.
[29] R. C. Dunbar, *J. Phys. Chem. A* **2002**, *106*, 7328–7337.
[30] J. Oomens, D. T. Moore, G. von Helden, G. Meijer, R. C. Dunbar, *J. Am. Chem. Soc.* **2004**, *126*, 724–725.
[31] D. T. Moore, J. Oomens, J. R. Eyler, G. von Helden, G. Meijer, R. C. Dunbar, *J. Am. Chem. Soc.* **2005**, *127*, 7243–7254.
[32] N. C. Polfer, R. C. Dunbar, J. Oomens, *J. Am Soc. Mass Spectrom.* **2007**, *18*, 512–516.
[33] *Gaussian 03W, Version 6.0*, M. J. Frisch, G. W. Trucks, H. B. Schlegel, G. E. Scuseria, M. A. Robb, J. R. Cheeseman, J. A. Montgomery, Jr., T. Vreven, K. N. Kudin, J. C. Burant, J. M. Millam, S. S. Iyengar, J. Tomasi, V. Barone, B. Mennucci, M. Cossi, G. Scalmani, N. Rega, G. A. Petersson, H. Nakatsuji, M. Hada, M. Ehara, K. Toyota, R. Fukuda, J. Hasegawa, M. Ishida, T. Nakajima, Y. Honda, O. Kitao, H. Nakai, M. Klene, X. Li, J. E. Knox, H. P. Hratchian, J. B. Cross, C. Adamo, J. Jaramillo, R. Gomperts, R. E. Stratmann, O. Yazyev, A. J. Austin, R. Cammi, C. Pomelli, J. W. Ochterski, P. Y. Ayala, K. Morokuma, G. A. Voth, P. Salvador, J. J. Dannenberg, V. G. Zakrzewski, S. Dapprich, A. D. Daniels, M. C. Strain, O. Farkas, D. K. Malick, A. D. Rabuck, K. Raghavachari, J. B. Foresman, J. V. Ortiz, Q. Cui, A. G. Baboul, S. Clifford, J. Cioslowski, B. B. Stefanov, G. Liu, A. Liashenko, P. Piskorz, I. Komaromi, R. L. Martin, D. J. Fox, T. Keith, M. A. Al-Laham, C. Y. Peng, A. Nanayakkara, M. Challacombe, P. M. W. Gill, B. Johnson, W. Chen, M. W. Wong, C. Gonzalez, J. A. Pople, Gaussian, Inc., Pittsburgh PA, **2003**.
[34] *Infrared Spectra* NIST Chemistry WebBook, NIST Standard Reference Database Number 69 (Eds.: P. J. Linstrom, W. G. Mallard), **2003**, *National Institute of Standards and Technology*, Gaithersburg MD, 20899 (http://webbook.nist.gov).
[35] P. B. Armentrout, M. T. Rodgers, *J. Phys. Chem. A* **2000**, *104*, 2238–2247.
[36] P. Wang, C. Wesdemiotis, C. Kapota, G. Ohanessian, *J. Am. Soc. Mass Spectrom.* **2007**, *18*, 541–552.
[37] B. A. Cerda, S. Hoyau, G. Ohanessian, C. Wesdemiotis, *J. Am. Chem. Soc.* **1998**, *120*, 2437–2448.
[38] M. Kish, C. Wesdemiotis, G. Ohanessian, *J. Phys. Chem. B* **2004**, *108*, 3086–3091.
[39] C. Kapota, G. Ohanessian, *Phys. Chem. Chem. Phys.* **2005**, *7*, 3744–3755.
[40] C. H. S. Wong, N. L. Ma, C. W. Tsang, *Chem. Eur. J.* **2002**, *8*, 4909–4918.
[41] M. Benzakour, M. McHarfi, A. Cartier, A. Daoudi, *J. Mol. Struc. Theochem* **2004**, *710*, 169–174.
[42] S. Abirami, C. H. S. Wong, C. W. Tsang, N. L. Ma, N. K. Goh, *J. Mol. Struc. Theochem* **2005**,*729*, 193–202.
[43] B. B. Koleva, T. Kolev, S. Y. Zareva, M. Spiteller, *J. Mol. Struct.* **2007**, *831*, 165–173.
[44] R. M. Moision, P. B. Armentrout, *J. Phys. Chem. A* **2002**, *106*, 10350–10362.
[45] R. M. Moision, P. B. Armentrout, *Phys. Chem. Chem. Phys.* **2004**, *6*, 2588–2599.
[46] T. Steiner, G. Koellner, *J. Mol. Biol.* **2001**, *305*, 535–557.

Received: October 17, 2007
Published online on February 21, 2008

